COMPARISON OF POWER PULSES FROM HOMOGENEOUS AND TIME-AVERAGE-EQUIVALENT MODELS *

T.K. De and B. Rouben

AECL
Sheridan Science and Technology Park
2251 Speakman Drive
Mississauga, Ontario
Canada L5K 1B2

ABSTRACT

The time-average-equivalent model is an "instantaneous" core model designed to reproduce the same three dimensional power distribution as that generated by a time-average model. However it has been found that the time-average-equivalent model gives a full-core static void reactivity about 8% smaller than the time-average or homogeneous models. To investigate the consequences of this difference in static void reactivity in time dependent calculations, simulations of the power pulse following a hypothetical large-loss-of-coolant accident were performed with a homogeneous model and compared with the power pulse from the time-average-equivalent model.

The results show that there is a much smaller difference in peak dynamic reactivity than in static void reactivity between the two models. This is attributed to the fact that voiding is not complete, but also to the retardation effect of the delayed-neutron precursors on the dynamic flux shape. The difference in peak reactivity between the models is 0.06 milli-k. The power pulses are essentially the same in the two models, because the delayed-neutron fraction in the time-average-equivalent model is lower than in the homogeneous model, which compensates for the lower void reactivity in the time-average-equivalent model.

INTRODUCTION

CERBERUS is the finite-difference neutron kinetics code used at AECL to solve the time-dependent diffusion equation in two energy groups (fast and thermal). CERBERUS exists as an independent stand-alone code, but it has also been integrated in RFSP, which is a code used to do neutronics calculations for CANDU reactors. However there is a difference in the modelling detail which can be accommodated by these two versions. The stand-alone CERBERUS allows a limited number (ca. 100) of "fuel types" and is therefore mainly used with a "homogeneous" model, which is similar to the "time-average" model (properties are averaged over a range of irradiation) but with axially uniform properties, i.e. along any channel the properties of the bundles are uniform. Furthermore this code version allows only one set of delayed neutron fractions, which must therefore be averaged over the entire core.

* This work was funded by COG WP25, WPIR 2506.

The *CERBERUS module of RFSP is computationally much more sophisticated. It allows more detailed, complex and realistic models. It can handle different fuel properties at each fuel bundle in the core (e.g. 4560 bundles in the CANDU 6 reactor core). Also the delayed-neutron fractions can be bundle-specific and therefore need not be averaged. This version is however restricted to models of the "instantaneous type", where each bundle has a single value of irradiation. It cannot handle time-average or homogeneous models, where properties are averaged over a range of irradiation.

The *CERBERUS module can therefore be executed on "snapshot" core model, or on the time-average-equivalent model, which is an instantaneous model designed to give the same power distribution as the time-average model. John Pitre has documented the method for constructing the time-average-equivalent (TAE) instantaneous-irradiation model within RFSP. This model is designed to be neutronically equivalent to the time-average model in most respects. However it has been seen that the value of static full-core void reactivity in the TAE model is about 8% smaller than in the time-average model or in the homogeneous model (which is similar to the time-average model but with axially uniform lattice properties).

The difference in void reactivity can be traced to the following cause. The lattice nuclear cross sections in the time-average and homogeneous models are calculated as averages over irradiation ω. The average properties have contributions from values of irradiation near zero (i.e. fresh fuel). Because void reactivity is high for fresh fuel, this increases the void reactivity in these models. In the time-average-equivalent model, each bundle has properties calculated at an instantaneous value of irradiation corresponding approximately to the mid-range of the irradiation experienced at that location. As a consequence, low values of ω do not contribute to the void reactivity in this model, resulting in a lower void reactivity.

It is important to know the consequences of this difference in void reactivity on the power pulse following a hypothetical large-loss-of-coolant accident (LOCA). To investigate this, kinetics simulations of the power pulse following a hypothetical large LOCA in the CANDU 6 reactor have been performed in two different ways:

a) using a "homogeneous" irradiation model together with the self-standing CERBERUS kinetics code, and

b) using the time-average-equivalent instantaneous model in the history based methodology in the *CERBERUS module of RFSP.

This document presents the methodology used and the results of these simulations.

METHODOLOGY

The analysis is performed for a 100% pump-suction break from an initial power of 103% FP with a nominal initial neutron flux distribution. The calculation is done up to 5 seconds after the break. The thermalhydraulics data (coolant density, coolant temperature and fuel temperature) for both the time-average-equivalent model and the homogeneous model is obtained with the code CATHENA (Reference 1). Also the same time steps are used in both models, including the SDS1 (shutoff rods) actuation time. In both models a coolant purity of 95.64% is used in the LOCA.

The power pulse is terminated by SDS1 actuation. Figure 1 gives a top view of the reactor showing the position of the 28 shutoff rods. Rods S1 and S5 are assumed non operational (i.e. they do not drop into the core when SDS1 is actuated). The remaining 26 rods are the least effective set. The shutoff rods are of two lengths. Rods S5, S8, S9, S13, S14, S15, S16, S20, S21 and S24 are the shorter ones, while the remaining 18 rods are longer. The rods are normally parked above the core with their upper ends all at the same height, and the bottom of the long rods about 13 feet above the reactor horizontal midplane. The long shutoff rods (Figure 2) are modelled as 18 lattice pitches long (514.35 cm) i.e 26.04 cm shorter than in reality. The short rods are modelled as 17 lattice pitches long (485.78 cm) i.e. 1.9 cm shorter than their actual length.

The shutoff-rod-drop characteristics used are shown in Table 1. The relative position of the long and short rods is kept unchanged during the drop into the core, i.e. all the rods are assumed to drop with the same velocity.

HOM Model

The homogeneous-irradiation (HOM) model, described below, is used instead of the full time-average model because, as noted earlier, the self-standing CERBERUS code cannot handle more than a limited number (ca. 100) of different sets of lattice properties. However it has been seen, that the homogeneous model and the time-average model produce essentially the same value of static void reactivity (within 0.1 milli-k).

In the HOM model, lattice properties are calculated using the reaction-rate-average option in the cell code POWDERPUFS-V, and the lattice properties are uniform throughout a channel. The nuclear cross sections are averaged over the interval $(0,\omega_{exit})$, where ω_{exit} is the exit irradiation value assumed for that channel. For instance the thermal absorption cross section, Σ_{a2}, in the homogeneous model is:

$$\sum\nolimits_{a2}^{hom.} = \frac{1}{\omega_{exit}} \int_0^{\omega_{exit}} \sum\nolimits_{a2} (\omega) d\omega$$

Note: The time-average model is similar to the homogeneous model, except that in the time-average model the lattice properties are not uniform over the channel, but are averaged for each bundle over a specific irradiation interval $(\omega_{in},\omega_{out})$, where ω_{in} and ω_{out} are respectively the irradiation values of the fuel when it enters the particular bundle location and when it exits from that location.

The core of the HOM model is subdivided radially into two irradiation zones, inner core and outer core, as shown in Figure 3. To account for differences in thermalhydraulics data from channel to channel, but taking into account the limitations of the self-standing CERBERUS, the ten thermalhydraulics channel types are collapsed to seven (see Figure 4).

In Figure 4 the core view is from the channel fixed end of the core. Coolant flow for channel types 1 to 5, which represent the channels of the critical core pass of the broken loop, is into the paper (i.e. from channel fixed end to channel free end). Channel type 6 represents all 95 channels of the non-critical core pass of the broken loop. The coolant flow here is out of paper (i.e. from the channel free end to the channel fixed end). Channel type 7 represents all 180 channels of the unbroken loop. In the axial direction lattice properties are averaged over 2 consecutive bundles in channel types 1 to 5, and over 3 consecutive bundles in channel types 6 and 7. These lattice properties are calculated by flux-squared weighting of the coolant densities, fuel temperatures and coolant temperatures of the bundles from the ten-channel thermalhydraulics model shown in Figure 5.

In the HOM model, the delayed-neutron data, consisting of delayed-neutron fractions, decay constants and group velocities, is uniform over the entire core. This data is calculated at an effective average exit irradiation of 1.734 n/kb (see Figure 3). The effective total delayed fraction is 0.00586.

The HOM model has 48, 30 and 34 meshes in the x, y and z directions. The spatial grid of the final model in the x-z plane, together with the shutoff rods, is shown in Figure 1.

TAE Model

The time-average-equivalent (TAE) model is obtained by running the *TAVEQUIV module of the code RFSP. This module creates an instantaneous core model which matches the time-average power distribution. The instantaneous irradiation for each bundle is calculated as follows. First the time-average k-infinity value for each bundle is determined from the time-average properties for that bundle. Then using the relationship between k-infinity and the instantaneous irradiation, a value of the irradiation is determined by interpolation in such a way that the instantaneous k-infinity matches the time average k-infinity value for that bundle.

The lattice properties are calculated with the *POWDERPUFS-V module in RFSP. The ten channel types of the thermalhydraulics model (Figure 5) are used. In the axial direction, in each channel type, the lattice properties are calculated independently for each of the twelve bundle positions. The *CERBERUS module in RFSP is used to perform the LOCA analysis.

The delayed-neutron fractions, decay constants and group velocities are calculated directly within the RFSP code. In the TAE model the delayed-neutron fraction is not averaged, but varies from bundle to bundle according to the bundle irradiation. However, the effective (core-average) total delayed fraction calculated for the TAE model is 0.00553. This is about 5% smaller than the value in the HOM model. The reason for this difference is similar to the reason for the difference in void reactivity: low values of irradiation, which give a higher delayed fraction, contribute more in the time-average or homogeneous model than in the instantaneous model.

The TAE model has 48, 36 and 32 meshes in the x, y and z directions. The difference from the HOM model in the number of mesh lines in the y and z directions was judged minor and not likely to be the origin of major differences in the calculated power pulse.

DISCUSSION OF THE RESULTS

Reactivity

Table 2 and Figure 6 show the dynamic reactivity versus time calculated with the TAE and HOM models. As expected, the reactivity is slightly higher in the HOM model. However, the difference is very small. At the beginning of the transient, the small difference is due to the relatively small amount of voiding. Further into the transient, when the voiding increases, the difference in reactivity remains small. This is due to the fact that in the CERBERUS methodology the reactivity is properly calculated with the dynamic (and not with the static) flux shape; the retardation effect of the delayed-neutron precursors reduces the difference in void reactivity.

The peak reactivity in the TAE Model is 3.25 milli-k, compared to 3.31 milli-k in the HOM model. The difference is only 0.06 milli-k (less than 2%). After SDS1 is actuated, negative reactivity is very quickly introduced. At 2.08 seconds after the break, when the shutoff rods are fully in core, the system reactivity reaches a value of –76.54 mk in the TAE model, compared to –74.86 mk for the HOM model. The difference of 1.68 mk, which remains almost constant for the rest of the analysis period, is attributed to two components: the different void reactivity and the difference in model geometry. It must be stressed that at this late stage of the transient, when the total reactor power has been reduced to a small value, the difference of 1.68 mk is not significant and has only a very small effect on the power pulse.

Total Reactor Power

Table 3 and Figure 7 show the total reactor power vs. time as calculated in the two models. In both models an initial power of 2123 MW (103% FP) at time 0 is used. After the break, the power in the TAE model rises slightly faster than in the HOM model. This is so even though the reactivity is slightly lower in the TAE model. The reason is the smaller delayed fraction in the TAE model.

By 0.875 second, when the shutoff rods enter the core, the total power is 4128 MW in the TAE model and 4043 MW in the HOM model (i.e. the total power in the TAE model is 2% higher). Both models reach peak power at time 1.095 seconds, with 4615 MW for the TAE model and 4477 MW for the HOM model. The TAE model thus gives a slightly higher peak power than the HOM model. From this time until 2.08 seconds the power drops rapidly in both models, more so in the TAE model, because of higher negative reactivity, so that the "tail" of the TAE power pulse is slightly lower than that from the HOM model, consistent with the reactivity difference. At 2.08 seconds after the break, the total power reduces to 323 MW and 315 MW in the HOM and the TAE models respectively. The difference however is still of the order of 2%.

Normalized Bundle Power Pulse For Selected Bundles

The normalized power pulse in two selected bundles is shown here. The bundles selected are those with:

a) the highest peak bundle power (largest instantaneous power), and

b) the maximum time-integrated bundle power at 5 seconds.

In each case the power pulse is normalized to an initial value of 1 by dividing the bundle power at any time by its power at time zero. The results are shown in Tables 4 and 5 as well as in Figures 8 and 9.

As with the total power, the bundle power pulse initially rises slightly faster in the TAE model than in the HOM model, due to the smaller delayed neutron fraction. After 1.372 seconds, the bundle power pulse in the TAE model drops below that in the HOM model, because of the slightly more negative system reactivity in the TAE model.

Relative value of largest integrated bundle power

In terms of absolute value, the largest time-integrated bundle power at 5 seconds is:

for HOM Model : 2.769 MW.s (bundle Q6-6)
for TAE Model : 2.838 MW.s (bundle O6-7)

The largest time-integrated bundle power in the TAE model is 2% higher than the HOM model. However the initial power of bundle Q6-6 (in HOM model) is 0.765 MW, compared to 0.801 MW for bundle O6-7 (in TAE model). Thus, for the "relative" power pulse, measured in terms of initial-power seconds, obtained by dividing the time integrated bundle power by the initial power of the bundle, the quantities are:

for HOM Model : 2.769/0.765 = 3.62 initial power seconds (bundle Q6-6)
for TAE Model : 2.838/0.801 = 3.54 initial power seconds (bundle O6-7)

The TAE value of maximum initial power seconds is therefore 2% smaller than the HOM value.

Maximum Energy Content of a Bundle

In this section we consider the total enthalpy, which would apply to the hot pin of a bundle initially at the license limit, if this bundle underwent the same power pulse as that experienced by the bundle with the largest integrated power (identified in the previous section). The initial stored energy in a hot pin containing 21.668 kg of UO_2 at full power can be obtained from the fuel temperature in the hot pin (assumed 1210°C) and the specific heat of UO_2 (0.32 J/g/°C). Using a room temperature of 20°C, we find:

Initial stored energy = 0.32 * (1210-20) = 380.8 J/g = 0.3808 kW.s/g

The power ratio between the hot pin and an average pin in the 37-element bundle is 1.131. Thus the power of the hot pin in a bundle at the license limit of 935 kW is given by:

Power of hot pin at full power = 935 / 37 * 1.131 = 28.58 kW
Also, the mass of fuel per pin = 21,668 / 37 = 586 g of UO_2.

Using the value of initial-power-seconds from the previous section, the maximum fuel enthalpy is:

for HOM Model : 0.3808 kW.s/g + 3.62 * 28.58 / 586 kW.s/g = 557.3 J/g
for TAE Model : 0.3808 kW.s/g + 3.54 * 28.58 / 586 kW.s/g = 553.4 J/g

Thus, in terms of total fuel enthalpy at 5 seconds, the TAE value is only about 0.8% smaller than the HOM value.

CONCLUSION

The power pulses generated by a time-average-equivalent model and a homogeneous model are compared. In spite of a smaller void reactivity in the time-average-equivalent model than in the time-average or the homogeneous model, kinetics calculations show that the power pulse in a time-average-equivalent model core is very close to that in a HOM model core. The smaller void reactivity is compensated for by a smaller delayed-neutron fraction.

Differences between the two models in all important quantities i.e. system reactivity, total reactor power pulse and normalized maximum bundle power pulse are very small, generally less than 2%. The difference in fuel enthalpy in the hot pin at 5 seconds is even smaller, less than 1%.

These results validate the use of the time-average-equivalent model instead of the time-average or homogeneous model in kinetics calculations of LOCA power pulses.

REFERENCES

1. B.N. Hanna, Editor, "CATHENA Input Reference", AECL-WL Report: RC-982-4/COG-93-140, Rev. 0.0.

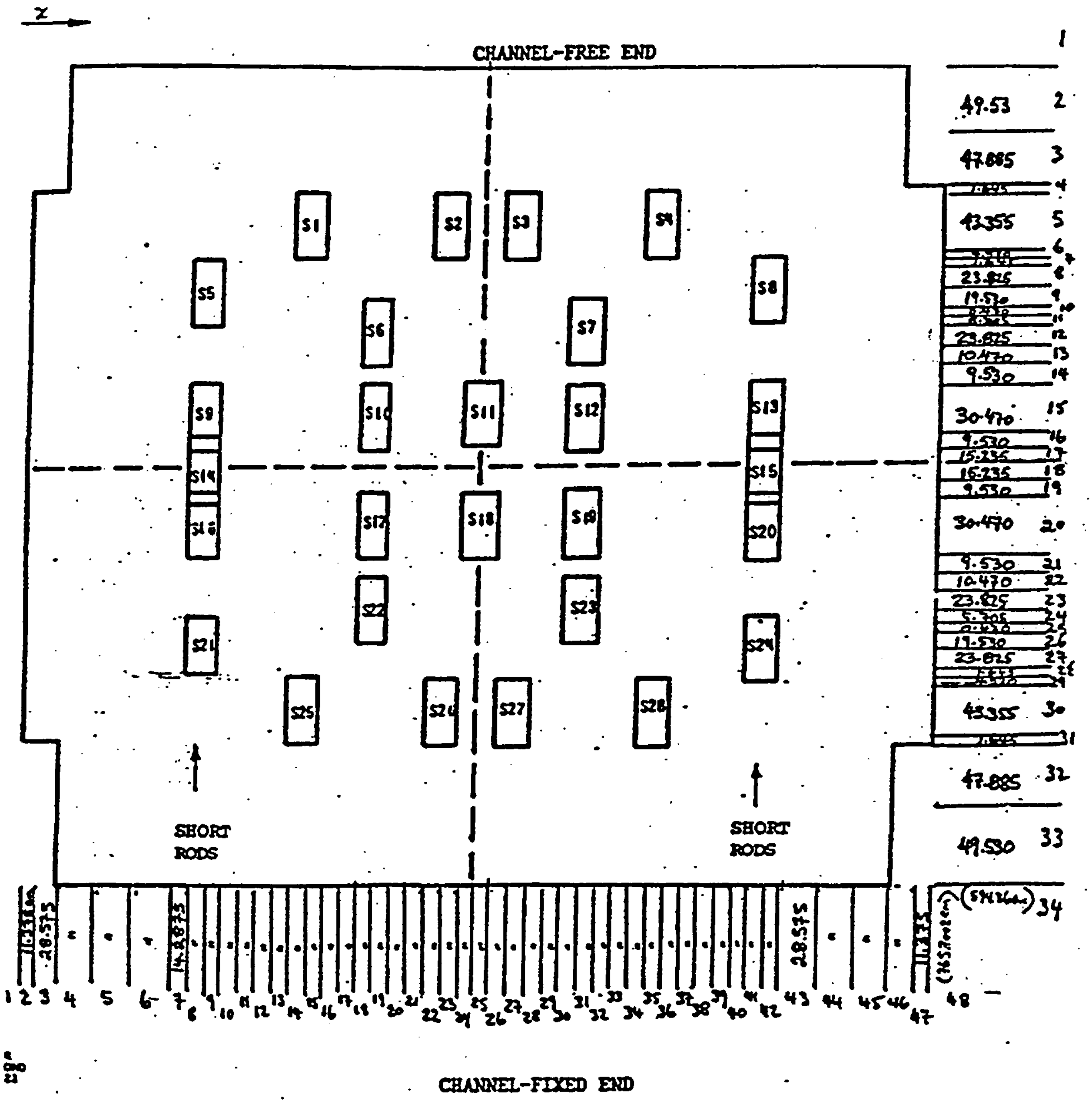

Figure 1 Top View of Reactor Showing Shutoff Rod Locations

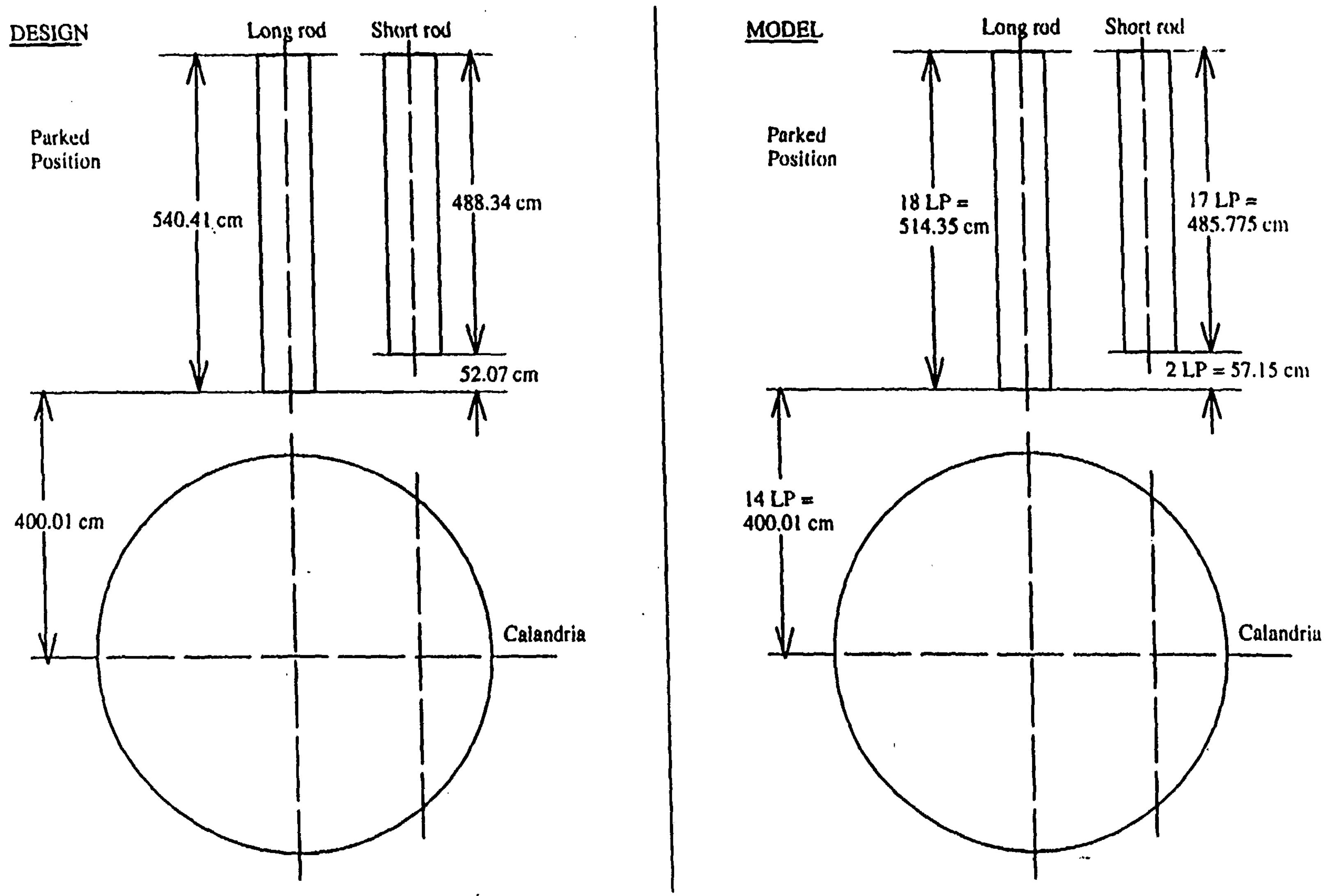

Figure 2 Shutoff Rod Length

	1	2	3	4	5	6	7	8	9	10	11	12	13	14	15	16	17	18	19	20	21	22
A									8	3	8	1	2	1								
B						8	3	8	3	8	3	2	1	2	1	2	1					
C					8	3	8	3	8	3	8	1	2	1	2	1	2	1				
D				8	3	8	3	8	3	4	3	2	1	2	1	2	1	2	1			
E			8	3	8	3	8	3	4	3	5	1	2	1	2	1	2	1	2	1		
F			3	8	3	4	3	4	3	4	3	2	1	2	1	2	1	2	1	2		
G		3	9	3	9	3	4	3	4	3	4	1	2	1	2	1	2	1	2	1	2	
H		9	3	9	3	4	3	4	3	4	3	2	1	2	1	2	1	2	1	2	1	
J	9	3	9	3	5	3	5	3	5	3	4	1	2	1	2	1	2	1	2	1	2	1
K	3	9	3	4	3	5	3	5	3	5	3	2	1	2	1	2	1	2	1	2	1	2
L	9	3	9	3	4	3	4	3	5	3	4	1	2	1	2	1	2	1	2	1	2	1
M	3	9	3	6	3	6	3	6	3	7	3	2	1	2	1	2	1	2	1	2	1	2
N	9	3	9	3	6	3	6	3	7	3	7	1	2	1	2	1	2	1	2	1	2	1
O	3	9	3	9	3	6	3	6	3	7	3	2	1	2	1	2	1	2	1	2	1	2
P		3	9	3	9	3	6	3	6	3	7	1	2	1	2	1	2	1	2	1	2	
Q		10	3	10	3	6	3	6	3	7	3	2	1	2	1	2	1	2	1	2	1	
R			10	3	10	3	6	3	6	3	7	1	2	1	2	1	2	1	2	1		
S			3	10	3	10	3	6	3	7	3	2	1	2	1	2	1	2	1	2		
T				3	10	3	10	3	6	3	7	1	2	1	2	1	2	1	2			
U					3	10	3	10	3	10	3	2	1	2	1	2	1	2				
V						3	10	3	10	3	10	1	2	1	2	1	2					
W									3	10	3	2	1	2								

Group 1: 95 channels Core pass 1 (intact loop)
Group 2: 95 channels Core pass 2 (intact loop)
Group 3: 95 channels Core pass 3 (broken loop)
Group 4: 16 channels Core pass 4 (broken loop)
Group 5: 8 channels Core pass 4 (broken loop)
Group 6: 15 channels Core pass 4 (broken loop)
Group 7: 9 channels Core pass 4 (broken loop)
Group 8: 16 channels Core pass 4 (broken loop)
Group 9: 16 channels Core pass 4 (broken loop)
Group 10: 15 channels Core pass 4 (broken loop)

Figure 3 Channel Types For Thermalhydraulics Analysis and for the Time-Average-Equivalent Model

01	02	03	04	05	06	07	08	09	10	11	12	13	14	15	16	17	18	19	20	21	22
								1.6940	1.6940	1.6940	1.6940	1.6940	1.6940								
					1.6940	1.6940	1.6940	1.6940	1.6940	1.6940	1.6940	1.6940	1.6940	1.6940	1.6940	1.6940					
				1.6940	1.6940	1.6940	1.6940	1.6940	1.6980	1.6980	1.6980	1.6980	1.6940	1.6940	1.6940	1.6940	1.6940				
			1.6940	1.6940	1.6940	1.6980	1.6980	1.6980	1.6980	1.6980	1.6980	1.6980	1.6980	1.6980	1.6980	1.6940	1.6940	1.6940			
		1.6940	1.6940	1.6940	1.6980	1.6980	1.6980	1.6980	1.6980	1.6980	1.6980	1.6980	1.6980	1.6980	1.6980	1.6980	1.6940	1.6940	1.6940		
		1.6940	1.6940	1.6980	1.6980	1.6980	1.6980	1.9190	1.9190	1.9190	1.9190	1.9190	1.9190	1.6980	1.6980	1.6980	1.6980	1.6940	1.6940		
	1.6940	1.6940	1.6980	1.6980	1.6980	1.9190	1.9190	1.9190	1.9190	1.9190	1.9190	1.9190	1.9190	1.9190	1.9190	1.6980	1.6980	1.6980	1.6940	1.6590	
	1.6940	1.6940	1.6980	1.6980	1.6980	1.9190	1.9190	1.9190	1.9190	1.9190	1.9190	1.9190	1.9190	1.9190	1.9190	1.6980	1.6980	1.6980	1.6940	1.6590	
1.6940	1.6940	1.6980	1.6980	1.6980	1.9190	1.9190	1.9190	1.9190	1.9190	1.9190	1.9190	1.9190	1.9190	1.9190	1.9190	1.9190	1.6980	1.6980	1.6980	1.6590	1.6590
1.6940	1.6940	1.6980	1.6980	1.6980	1.9190	1.9190	1.9190	1.9190	1.9190	1.9190	1.9190	1.9190	1.9190	1.9190	1.9190	1.9190	1.6980	1.6980	1.6980	1.6590	1.6590
1.6940	1.6940	1.6980	1.6980	1.6980	1.9190	1.9190	1.9190	1.9190	1.9190	1.9190	1.9190	1.9190	1.9190	1.9190	1.9190	1.9190	1.6980	1.6980	1.6980	1.6590	1.6590
1.6940	1.6940	1.6980	1.6980	1.6980	1.9190	1.9190	1.9190	1.9190	1.9190	1.9190	1.9190	1.9190	1.9190	1.9190	1.9190	1.9190	1.6980	1.6980	1.6980	1.6590	1.6590
1.6940	1.6940	1.6980	1.6980	1.6980	1.9190	1.9190	1.9190	1.9190	1.9190	1.9190	1.9190	1.9190	1.9190	1.9190	1.9190	1.9190	1.6980	1.6980	1.6980	1.6590	1.6590
1.6940	1.6940	1.6980	1.6980	1.6980	1.9190	1.9190	1.9190	1.9190	1.9190	1.9190	1.9190	1.9190	1.9190	1.9190	1.9190	1.9190	1.6980	1.6980	1.6980	1.6590	1.6590
	1.6940	1.6940	1.6980	1.6980	1.6980	1.9190	1.9190	1.9190	1.9190	1.9190	1.9190	1.9190	1.9190	1.9190	1.9190	1.6980	1.6980	1.6980	1.6940	1.6590	
	1.6940	1.6940	1.6980	1.6980	1.6980	1.9190	1.9190	1.9190	1.9190	1.9190	1.9190	1.9190	1.9190	1.9190	1.9190	1.6980	1.6980	1.6980	1.6940	1.6590	
		1.6940	1.6940	1.6980	1.6980	1.6980	1.6980	1.9190	1.9190	1.9190	1.9190	1.9190	1.9190	1.6980	1.6980	1.6980	1.6980	1.6940	1.6940		
		1.6940	1.6940	1.6940	1.6980	1.6980	1.6980	1.6980	1.6980	1.6980	1.6980	1.6980	1.6980	1.6980	1.6980	1.6980	1.6940	1.6940	1.6940		
			1.6940	1.6940	1.6940	1.6980	1.6980	1.6980	1.6980	1.6980	1.6980	1.6980	1.6980	1.6980	1.6980	1.6940	1.6940	1.6940			
				1.5030	1.5030	1.5030	1.5030	1.5030	1.5030	1.5030	1.5030	1.5030	1.5030	1.5030	1.5030	1.5030	1.5030				
					1.4030	1.4030	1.4030	1.4030	1.4030	1.4030	1.4030	1.4030	1.4030	1.4030	1.4030	1.4030					
								.9900	.9900	.9900	.9900	.9900	.9900								

Average Exit Irradiation at Inner Core (no. of Channels 124) = 1.9190 n/kb

Average Exit Irradiation at Outer Core (no. of Channels 256) = 1.65316 n/kb

Average Exit Irradiation for the Entire Core

= (1.9190 * 124 + 1.65316 * 256) / (124 + 256)
= 1.7399 n/kb

Figure 4 Exit Irradiation

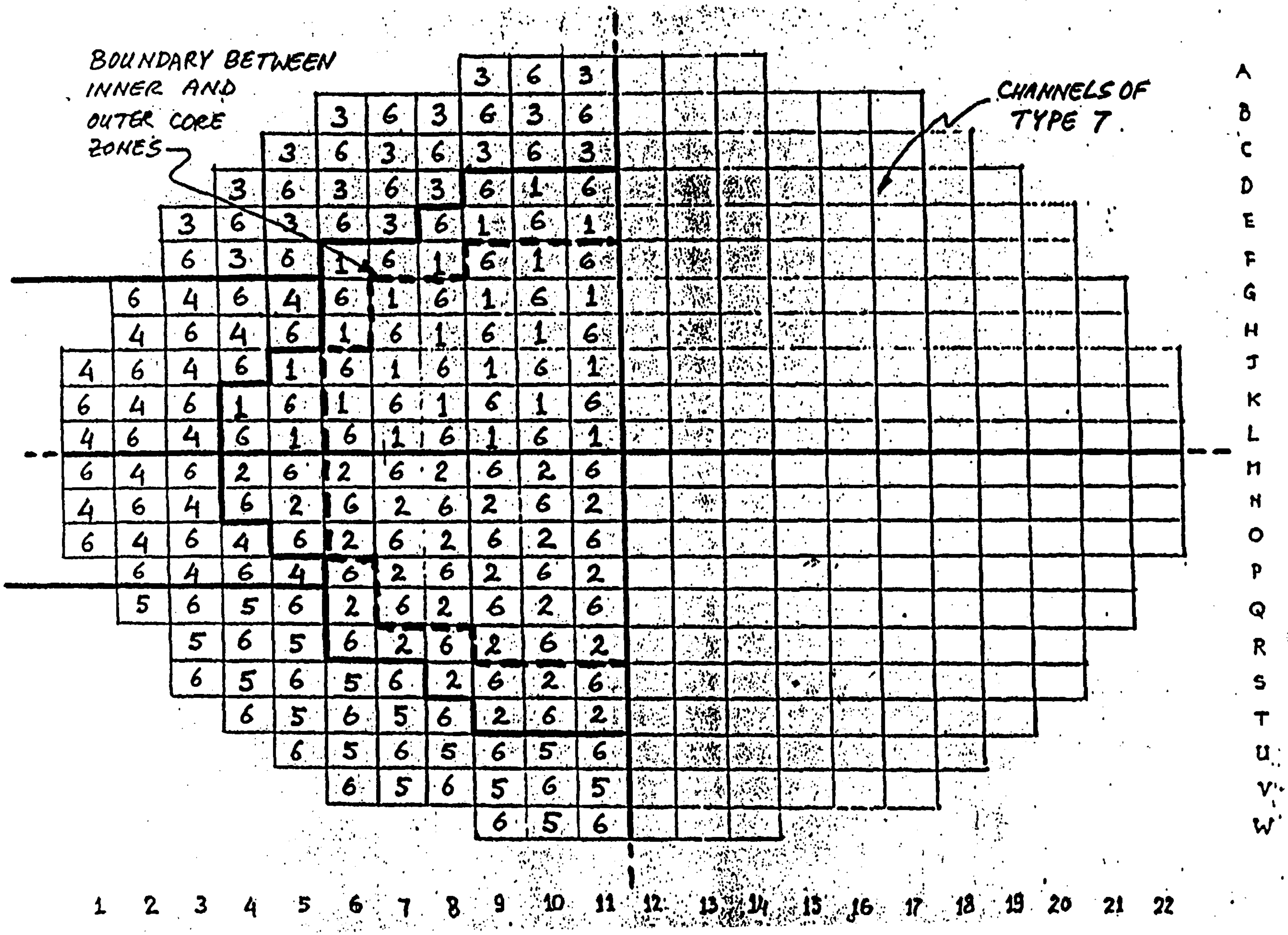

Figure 5 Channel Types for the Homogeneous Model

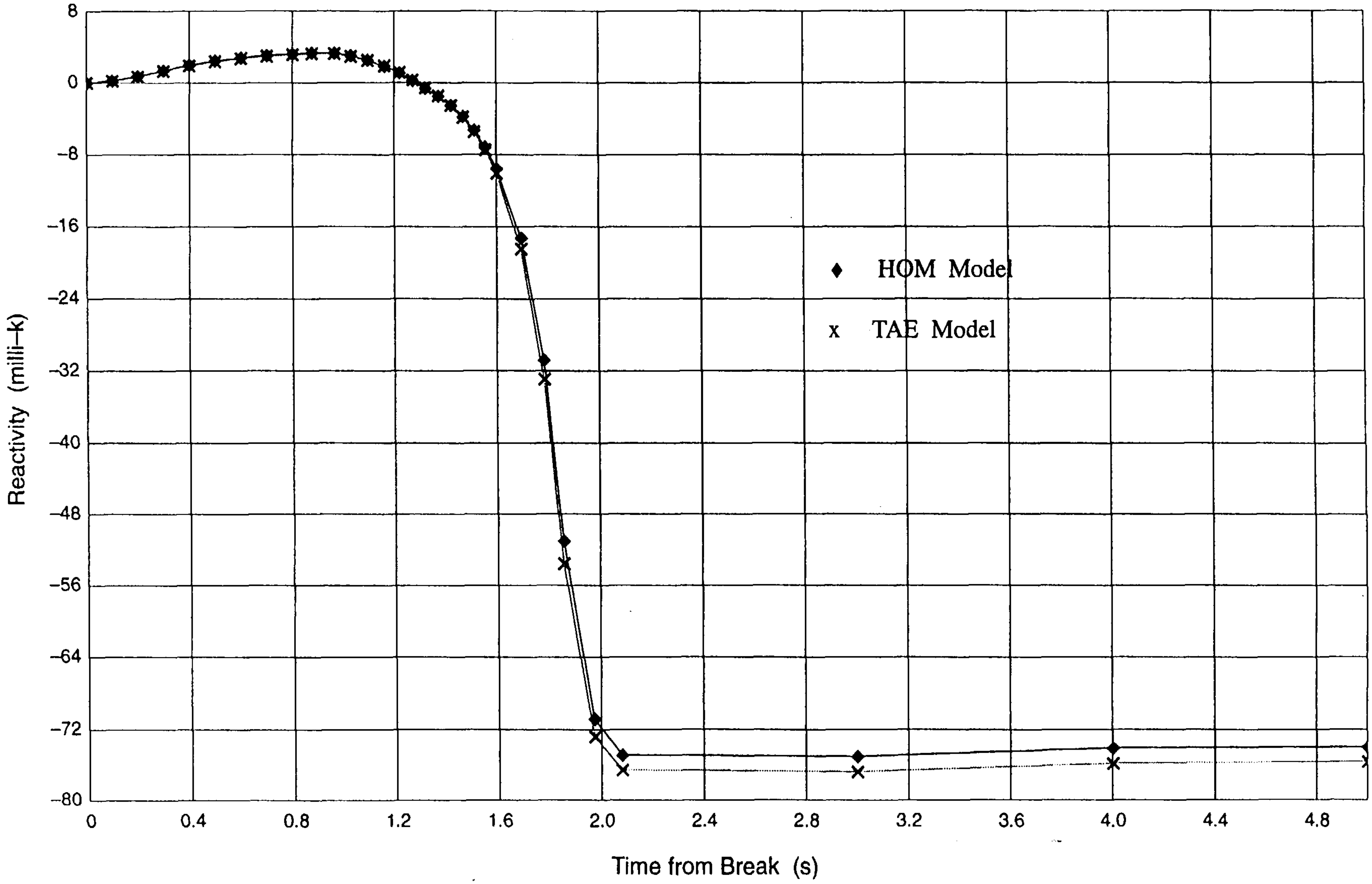

Figure 6 Comparison of System Reactivity During the LOCA

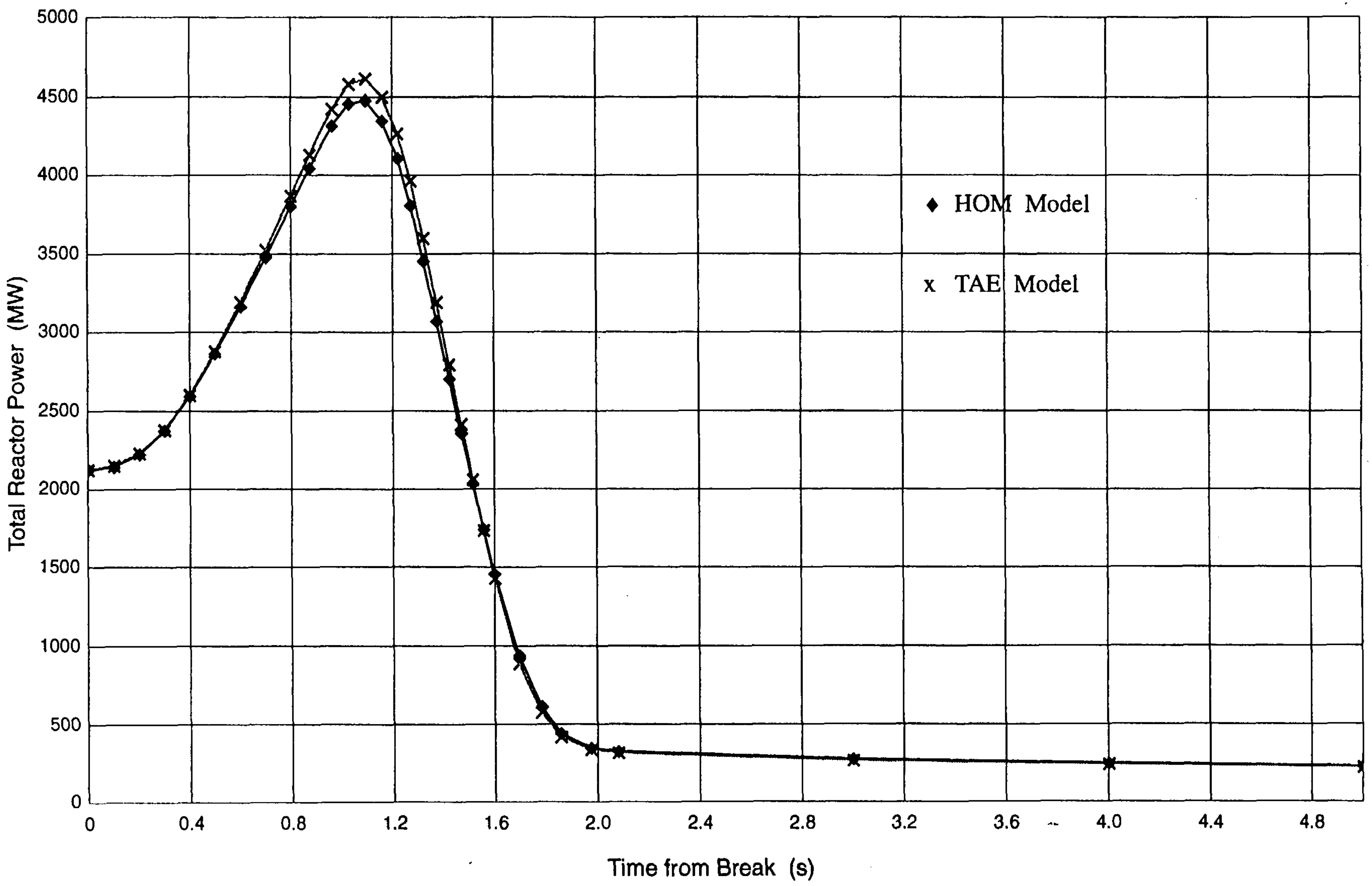

Figure 7 Comparison of Total Reactor Power

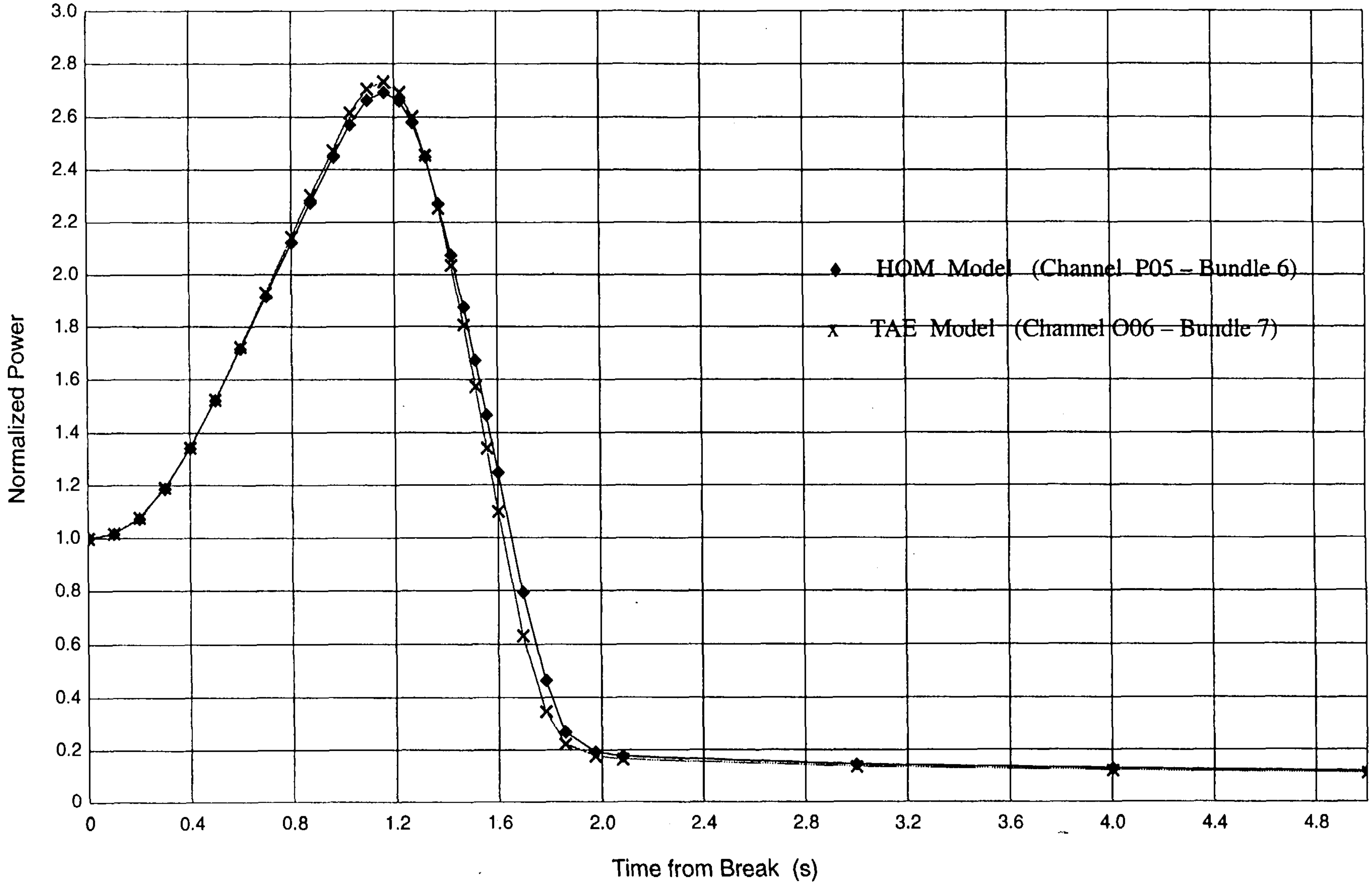

Figure 8 Comparison of Normalized Power for Bundle with Largest Instantaneous Power

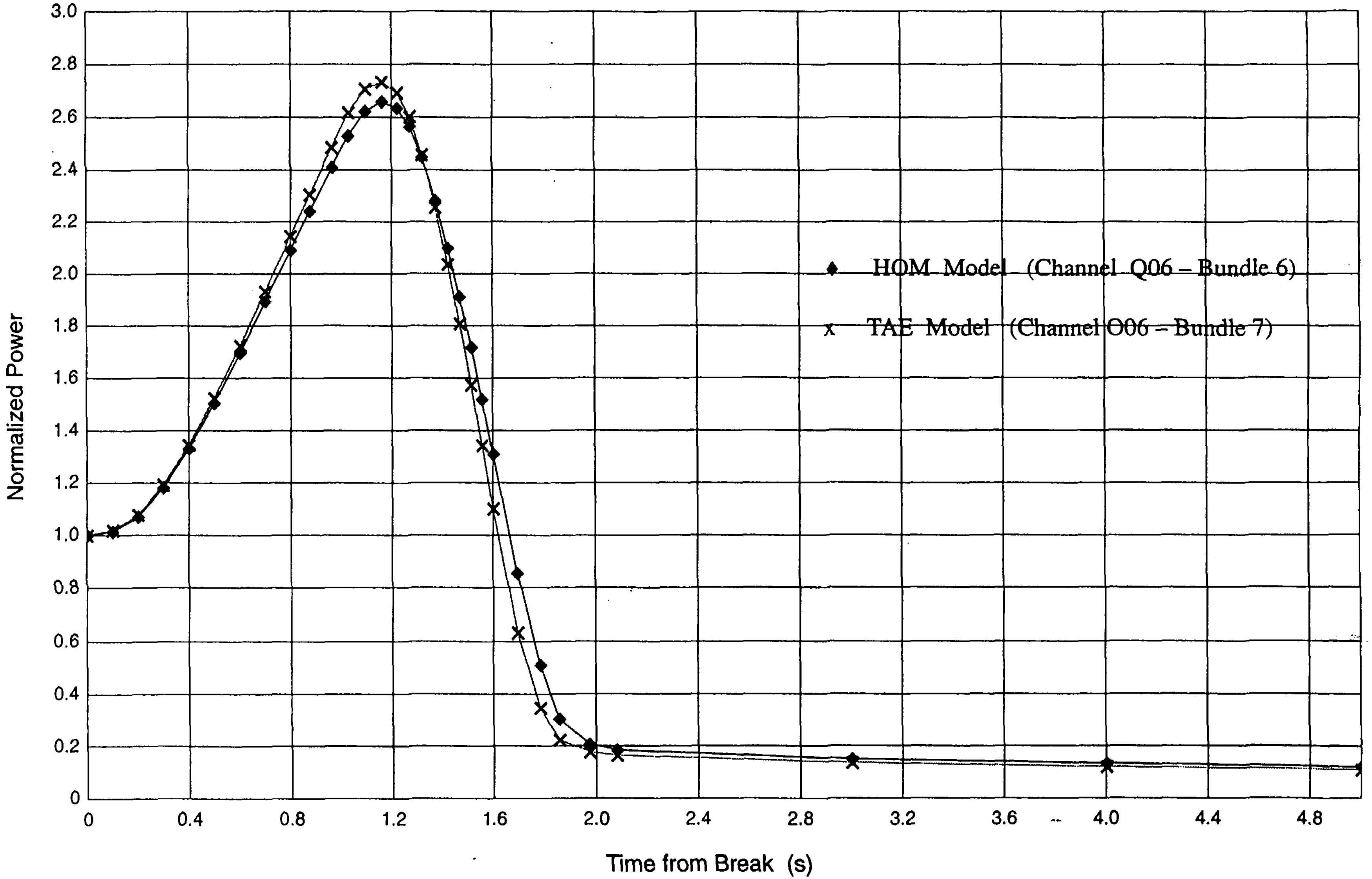

Figure 9 Comparison of Normalized Power for Bundle with Largest Stored Energy

Table 1
Position of the Bottom of Long Shutoff Rod From Calandria Centreline Versus Time

Time from break (s)	*Distance from reactor horizontal midplane* (cm)
0.000	Out of Core
0.100	Out of Core
0.200	Out of Core
0.300	Out of Core
0.400	Out of Core
0.500	Out of Core
0.600	Out of Core
0.700	Out of Core
0.800	Out of Core
0.875	371.475
0.964	342.900
1.029	314.325
1.095	285.750
1.161	257.175
1.221	228.600
1.272	200.025
1.321	171.450
1.372	142.875
1.421	114.300
1.468	85.725
1.531	57.150
1.556	28.575
1.600	0
1.695	-57.150
1.783	-114.300
1.856	-171.450
1.973	-228.600
2.080	-257.175

Table 2
Reactivity Transient Following Break

Case No.	Time from Break (s)	Reactivity (milli-k)	
		HOM	TAE
1	0.000	0.000	0.000
3	0.100	0.212	0.206
4	0.200	0.729	0.697
5	0.300	1.389	1.329
6	0.400	1.981	1.918
7	0.500	2.455	2.394
8	0.600	2.794	2.732
9	0.700	3.040	2.975
10	0.800	3.220	3.151
11	0.875	3.310	3.241
12	0.964	3.314	3.252
13	1.029	3.030	2.954
14	1.095	2.524	2.498
15	1.161	1.867	1.888
16	1.221	1.101	1.149
17	1.272	0.236	0.304
18	1.321	-0.629	-0.571
19	1.372	-1.505	-1.451
20	1.421	-2.513	-2.518
21	1.468	-3.757	-3.809
22	1.513	-5.263	-5.446
23	1.556	-7.167	-7.447
24	1.600	-9.583	-10.08
25	1.695	-17.26	-18.48
26	1.783	-30.82	-32.94
27	1.856	-51.04	-53.59
28	1.973	-70.81	-72.76
29	2.080	-74.86	-76.54
30	3.000	-75.02	-76.78
31	4.000	-74.08	-75.80
32	5.000	-73.97	-75.62

Table 3
Total Reactor Power

Case No.	Time from Break (s)	Total Power (MW)	
		HOM	TAE
1	0.000	2123	2123
3	0.100	2142	2149
4	0.200	2223	2229
5	0.300	2375	2379
6	0.400	2594	2600
7	0.500	2863	2877
8	0.600	3163	3191
9	0.700	3478	3523
10	0.800	3800	3867
11	0.875	4043	4128
12	0.964	4314	4423
13	1.029	4456	4579
14	1.095	4477	4615
15	1.161	4348	4501
16	1.221	4104	4265
17	1.272	3805	3963
18	1.321	3455	3600
19	1.372	3069	3190
20	1.421	2702	2792
21	1.468	2357	2414
22	1.513	2036	2059
23	1.556	1740	1735
24	1.600	1456	1428
25	1.695	941	890
26	1.783	615	578
27	1.856	440	419
28	1.973	346	336
29	2.080	323	315
30	3.000	273	265
31	4.000	245	239
32	5.000	225	220

Table 4
Normalized Power for Bundle with Largest Instantaneous Power

Case No.	Time from Break (s)	Highest Bundle Power (kW)		Bundle Power Ratio	
		HOM	TAE	HOM	TAE
1	0.000	766	801.5	1.000	1.000
3	0.100	779	816.9	1.017	1.019
4	0.200	823	864.4	1.074	1.078
5	0.300	910	955.4	1.188	1.192
6	0.400	1028	1077.5	1.342	1.344
7	0.500	1166	1222.3	1.522	1.525
8	0.600	1315	1381.5	1.716	1.723
9	0.700	1469	1548.3	1.917	1.931
10	0.800	1626	1718.6	2.122	2.144
11	0.875	1743	1847.3	2.275	2.304
12	0.964	1876	1966.8	2.449	2.454
13	1.029	1970	2096.9	2.571	2.616
14	1.095	2040	2168.1	2.663	2.705
15	1.161	2063	2189.7	2.693	2.732
16	1.221	2038	2157.7	2.660	2.692
17	1.272	1976	2085.1	2.579	2.601
18	1.321	1877	1969.1	2.450	2.456
19	1.372	1739	1807.2	2.270	2.254
20	1.421	1590	1631.8	2.075	2.036
21	1.468	1437	1449.0	1.876	1.807
22	1.513	1281	1261.1	1.672	1.574
23	1.556	1124	1075.7	1.467	1.342
24	1.600	957	882.6	1.249	1.101
25	1.695	609	507.9	0.795	0.633
26	1.783	357	279.5	0.466	0.348
27	1.856	207	180.2	0.270	0.224
28	1.973	148	142.2	0.193	0.177
29	2.080	135	132.6	0.176	0.165
30	3.000	111	109.0	0.145	0.136
31	4.000	98	96.9	0.128	0.120
32	5.000	89	88.3	0.116	0.110

Table 5
Normalized Power for Bundle with Largest Stored Energy

Case No.	Time from Break (s)	Highest Bundle Power (kW)		Bundle Power Ratio	
		HOM	TAE	HOM	TAE
1	0.000	766	801.5	1.000	1.000
3	0.100	777	816.9	1.014	1.019
4	0.200	820	864.4	1.070	1.078
5	0.300	905	955.4	1.181	1.192
6	0.400	1020	1077.5	1.331	1.344
7	0.500	1154	1222.3	1.506	1.525
8	0.600	1299	1381.5	1.695	1.723
9	0.700	1450	1548.3	1.893	1.931
10	0.800	1602	1718.6	2.091	2.144
11	0.875	1716	1847.3	2.240	2.304
12	0.964	1845	1966.8	2.408	2.454
13	1.029	1937	2096.9	2.528	2.616
14	1.095	2008	2168.1	2.621	2.705
15	1.161	2036	2189.7	2.658	2.732
16	1.221	2018	2157.7	2.634	2.692
17	1.272	1965	2085.1	2.565	2.601
18	1.321	1875	1969.1	2.447	2.456
19	1.372	1748	1807.2	2.282	2.254
20	1.421	1608	1631.8	2.099	2.036
21	1.468	1464	1449.0	1.911	1.807
22	1.513	1315	1261.1	1.716	1.574
23	1.556	1164	1075.7	1.519	1.342
24	1.600	1003	882.6	1.309	1.101
25	1.695	655	507.9	0.855	0.633
26	1.783	392	279.5	0.511	0.348
27	1.856	234	180.2	0.305	0.224
28	1.973	159	142.2	0.207	0.177
29	2.080	142	132.6	0.185	0.165
30	3.000	115	109.0	0.150	0.136
31	4.000	102	96.9	0.133	0.120
32	5.000	93	88.3	0.121	0.110